

Reactions of Palladium(II) Chloride with Monoiminoacenaphthenones

A. N. Lukoyanov^a, N. F. Romashev^{b, *}, V. I. Komlyagina^{b, c}, V. V. Kokovkin^b,
A. V. Cherkasov^a, and A. L. Gushchin^{b, **}

^a Razuvaev Institute of Organometallic Chemistry, Russian Academy of Sciences, Nizhny Novgorod, Russia

^b Nikolaev Institute of Inorganic Chemistry, Siberian Branch, Russian Academy of Sciences, Novosibirsk, Russia

^c Novosibirsk Research State University, Novosibirsk, Russia

*e-mail: nikolaj.romashev75@gmail.com

**e-mail: gushchin@niic.nsc.ru

Received July 14, 2023; revised July 29, 2023; accepted August 3, 2023

Abstract—The reaction of PdCl₂ with [2,6-diisopropylphenyl]iminoacenaphthenone (Dpp-mian) in dichloromethane affords compound [Pd(Dpp-mian)Cl₂]₂[Pd(Dpp-mian)₂Cl₂] (**I**). Complex **I** contains two structural units: [Pd(Dpp-mian)Cl₂] in which Dpp-mian coordinates to Pd(II) via the bidentate-chelate mode by the nitrogen and oxygen atoms and [Pd(Dpp-mian)₂Cl₂] where two Dpp-mian molecules are linked with palladium only via the nitrogen atom. The reaction of PdCl₂ with [4-methoxyphenyl]iminoacenaphthenone (4-MeOPh-mian) in dichloromethane is accompanied by the rearrangement of the ligand structure followed by the formation of the earlier described Pd(II) complex with 1,2-bis[4-methoxyphenyl]iminoacenaphthene (4-MeOPh-bian): [Pd(4-MeOPh-bian)Cl₂] (**II**) (CIF file CCDC no. 2280529). Compound **I** is synthesized for the first time and characterized by X-ray diffraction (XRD) (CIF file CCDC no. 2280528 (**I**)), phase XRD, elemental analysis, IR spectroscopy, and cyclic voltammetry.

Keywords: palladium, iminoacenaphthenones, XRD, complexes, synthesis, cyclic voltammetry

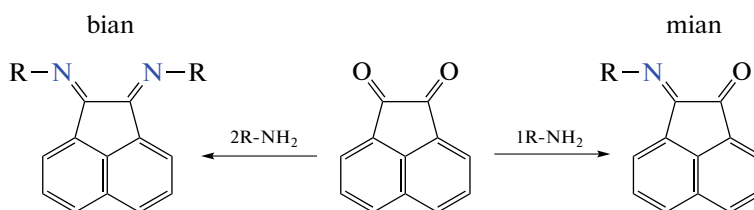
DOI: 10.1134/S1070328423601176

INTRODUCTION

Monoiminoacenaphthenones (mian) are referred to the class of redox-active ligands. They are the product of the partial condensation of acenaphthenequinone with one equivalent of aromatic amine [1–4] and are intermediates in the synthesis of bis(iminoacenaphthenes) (bian), which compose a well-known class of redox-active ligands, whose complexes found wide use in such areas as catalysis, bioinorganic chem-

istry, magnetochemistry, etc. [5–11]. Monoiminoacenaphthenones contain both carbonyl and imine functional groups conjugated with the naphthalene framework, which results in the unique coordination [12] and redox properties [1, 4].

The synthesis of monoiminoacenaphthenones (mian) and bis(iminoacenaphthenes) (bian) is shown in Scheme 1.



Scheme 1.

To this day, metal complexes with mian are studied rather piecemeal. For instance, according to the Cambridge Structural Database, 17 structurally characterized complexes with *d* elements are known [12–20]. The studies of the properties of the transition metal

complexes with the ligands of this class were initiated by Prof. T. Panda's research group [13, 16, 21]. On the one hand, a possibility of using the zinc complexes in the guanylation of carbodiimides and isocyanates with anilines was shown in this series of works. On the other

hand, complexes of platinum metals with mian are virtually unknown. Only two ruthenium complexes [Ru(Ph-mian)(Trpy)Cl](ClO₄) [22] and [Ru(Ph-mian)(Tpm)Cl](ClO₄) [19] were described. The Ru/bian and Ru/mian complexes were comparatively studied in the oxidation of alcohols and epoxidation of olefins. The reactivity of monoiminoacenaphthenones toward palladium was not studied. Only one Pd(II) complex with 2-((2,6-diisopropylphenyl)imino)-1-methyl-1,2-dihydroacenaphthyl-1-ol was mentioned. This complex is formed by the methylation of mono-(2,6-diisopropylphenyl)acenaphthenone (Dpp-mian) at the carbonyl carbon atom followed by the coordination of α -hydroxyimine to PdCl₂ [23].

In this work, the reactions of PdCl₂ with [2,6-diisopropylphenyl]iminoacenaphthenone and [4-methoxyphenyl]iminoacenaphthenone were carried out. As a result, new coordination compound [Pd(Dpp-mian)Cl₂]₂[Pd(Dpp-mian)₂Cl₂], which is the first example of the coordination of monoiminoacenaphthenone (in the given case, Dpp-mian) to palladium, was synthesized and structurally characterized, and its redox properties were studied by cyclic voltammetry (CV).

EXPERIMENTAL

The initial compounds Dpp-mian and 4-MeOPh-mian were synthesized using known procedures [1, 14]. Acenaphthenequinone (Sigma Aldrich, 99%) and PdCl₂ (Krastsvetmet) were used as received. Solvents were purified using standard procedures. IR spectra in a range of 4000–400 cm⁻¹ were recorded on a Scimitar FTS 2000 spectrometer for samples pressed in KBr pellets. Elemental analysis to C, H, N, S was conducted on a Euro EA 3000 instrument. Electrochemical measurements were carried out on an R-45Kh potentiostat-galvanostat (Elins, Russia) at room temperature in acetonitrile with 0.10 M Bu₄NPF₆ as a supporting electrolyte. The three-electrode cell used consisted of an indicative paste electrode, a silver chloride reference electrode filled with a KCl solution, and an auxiliary Pt electrode. The cell was described in detail [24–26]. A mixture of a carbon powder, a 10% aqueous Nafion dispersion, and an electroactive substance composed the paste. The component ratio based on the dry mixture was 100 : 6 : 3–7 mg. The potential sweep rate was 10 mV/s. Ferrocene with the potential $E_{1/2} = 0.43$ V (vs. Ag/AgCl) was used as an internal standard.

Synthesis of [Pd(Dpp-mian)Cl₂]₂[Pd(Dpp-mian)₂Cl₂] (I). A solution of [PdCl₂(CH₃CN)₂] (0.19 g, 0.75 mmol) in CH₂Cl₂ (10 mL) was poured to a solution of Dpp-mian (0.34 g, 1.0 mmol) in dichloromethane (10 mL). The resulting solution was left at room temperature for a day. As a result, a red-brown crystal-

line product of complex **I** was formed. The yield of the product was 0.48 g (93%). $T_{\text{decomp}} > 207^\circ\text{C}$.

The crystals suitable for XRD were prepared as follows: [PdCl₂(CH₃CN)₂] (0.05 g) was placed in one of the knees of an H-shaped tube (4 mm in diameter), the tube was filled with dichloromethane in such a way that no air bubbles remained in the tube, and crystalline Dpp-mian (0.1 g) was added to the second knee. The tube was tightly closed, and the substances were slowly mixed at room temperature. Crystals of complex **I** suitable for XRD were formed for 3 weeks in the medium part of the reaction tube.

For C₉₈H₉₆N₄O₄Cl₁₀Pd₃

Anal. calcd., %	C, 56.93	H, 4.68	N, 2.71
Found, %	C, 57.2	H, 4.87	N, 2.9

IR (KBr; ν , cm⁻¹): 3061 w, 2958 m, 2926 m, 2900 m, 2866 m, 1732 s, 1662 w, 1635 s, 1622 s, 1604 s, 1579 vs, 1489 m, 1465 m, 1435 m, 1419 m, 1384 m, 1363 m, 1328 w, 1300 m, 1274 m, 1265 m, 1219 m, 1178 w, 1151 w, 1120 m, 1099 w, 1072 w, 1056 w, 1045 w, 1029 m, 989 w, 956 w, 937 w, 916 m, 831 m, 800 m, 783 m, 773 s, 738 s, 715 m, 675 w, 634 w, 592 w, 568 w, 536 m, 516 w, 489 w, 466 w, 418 w, 405 w.

Synthesis of [Pd(4-MeOPh-bian)Cl₂] (II). The far knee of an H-shaped tube was filled with PdCl₂ (0.05 g, 0.28 mmol), and the tube was completely filled with acetonitrile. Then crystalline 4-MeOPh-mian (0.16 g, 0.56 mmol) was added, and the tube was sealed. Thus prepared sample was stored at room temperature without stirring for a month. Red crystals of complex **II** suitable for XRD were formed within this time in the medium part of the H-shaped tube. The yield of the product was 0.09 g (56%).

For C₂₆H₂₀N₂O₂PdCl₂

Anal. calcd., %	C, 54.8	H, 3.54	N, 4.9
Found, %	C, 54.5	H, 3.50	N, 5.0

IR (KBr; ν , cm⁻¹): 3444 br, 3192 m, 3120 m, 3055 w, 3018 w, 3003 w, 2960 w, 2945 w, 2897 w, 2833 w, 1635 m, 1598 s, 1502 vs, 1463 m, 1436 m, 1423 m, 1298 m, 1278 m, 1251 vs, 1176 m, 1166 m, 1151 m, 1105 m, 1080 w, 1033 s, 960 w, 920 w, 829 s, 806 w, 779 s, 761 w, 736 w, 723 w, 692 w, 651 w, 632 w, 559 w, 530 m, 493 w, 457 w, 428 w.

XRD of single crystals of compounds **I** (0.36 × 0.24 × 0.08 mm) and **II** (0.21 × 0.10 × 0.06 mm) was carried out on a Bruker D8 Quest diffractometer (MoK α radiation, ω scan mode, $\lambda = 0.71073$ Å) at $T = 100.0(2)$ K. Experimental sets of intensities were measured and integrated, an absorption correction was applied, and structure refinement was performed

using the APEX3 [27], SADABS [28], and SHELX [29] software.

Compound **I** ($C_{48}H_{46}Cl_2N_2O_2Pd$, $2C_{24}H_{23}Cl_2N-O Pd$, $2CH_2Cl_2$) crystallizes in the space group $P\bar{1}$ ($a = 8.5740(5)$, $b = 15.6553(9)$, $c = 17.4131(10)$ Å, $\alpha = 73.323(2)^\circ$, $\beta = 82.933(2)^\circ$, $\gamma = 87.795(2)^\circ$, $V = 2222.0(2)$ Å³, $Z = 1$, $\rho_{calc} = 1.545$ g/cm³, $\mu = 0.957$ mm⁻¹). Of 53731 measured reflections ($\theta_{max} = 26.06^\circ$), 8783 independent reflections ($R_{int} = 0.0459$) were used for structure solution using the dual-space algorithm [30] and subsequent refinement of 575 parameters by full-matrix least squares for F_{hkl}^2 in the anisotropic approximation for non-hydrogen atoms. After the final refinement, $wR_2 = 0.0599$ and $S(F^2) = 1.054$ for all reflections ($R_1 = 0.0301$ for all 7358 reflections satisfying the condition $F^2 > 2\sigma(F^2)$). The residual electron density maximum and minimum were 0.50/−0.64 e/Å³.

Compound **II** ($C_{26}H_{20}Cl_2N_2O_2Pd$, C_2H_3N) crystallizes in the space group $P2_1/n$ ($a = 12.0587(4)$, $b = 13.3433(5)$, $c = 15.9962(6)$ Å, $\beta = 106.2820(10)^\circ$, $V = 2470.61(15)$ Å³, $Z = 4$, $\rho_{calc} = 1.642$ g/cm³, $\mu = 1.000$ mm⁻¹). Of 127767 measured reflections ($\theta_{max} = 30.11^\circ$), 7258 independent reflections ($R_{int} = 0.0506$) were used for structure solution using the dual-space algorithm [30] and subsequent refinement of 328 parameters by full-matrix least squares for F_{hkl}^2 in the anisotropic approximation for non-hydrogen atoms. After the final refinement, $wR_2 = 0.0759$ and $S(F^2) = 1.051$ for all reflections ($R_1 = 0.0348$ for all 6017 reflections satisfying the condition $F^2 > 2\sigma(F^2)$). The residual electron density maximum and minimum were 1.46/−0.73 e/Å³.

All hydrogen atoms in compounds **I** and **II** were placed in the geometrically calculated positions and refined isotropically with the fixed thermal parameters $U(H)_{iso} = 1.2U(C)_{eq}$ ($U(H)_{iso} = 1.5U(C)_{eq}$ for methyl groups).

The structures of compounds **I** and **II** were deposited with the Cambridge Crystallographic Data Centre (CIF files CCDC nos. 2280528 (**I**) and 2280529 (**II**)) and are available at ccdc.cam.ac.uk/structures.

Phase XRD of compound **I** was carried out on a Shimadzu XRD-7000 diffractometer (CuK α radiation, Ni filter, OneSight linear detector, 3–40 2 θ range, increment 0.03° 2 θ , acquisition number 1 s per point). Samples for the study were prepared as follows: polycrystals were triturated in an agate mortar with heptane, and the prepared suspension was deposited on the polished side of a standard quartz cell. After heptane evaporated, the sample represented a thin smooth layer (thickness ~100 μ m).

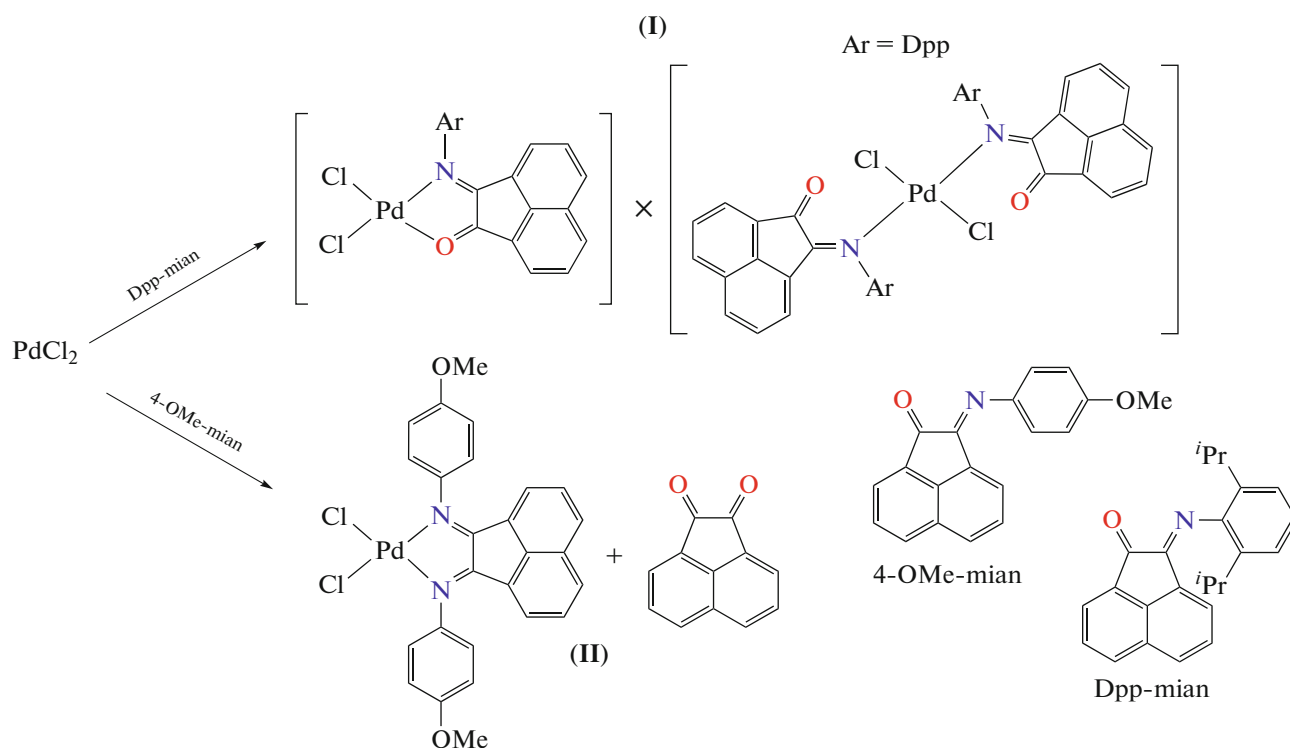
RESULTS AND DISCUSSION

The reaction of PdCl₂ with an acetonitrile excess followed by the treatment of the formed precipitate [Pd(CH₃CN)₂Cl₂] with a solution of Dpp-mian in dichloromethane gives compound [Pd(Dpp-mian)Cl₂]₂[Pd(Dpp-mian)₂Cl₂] (**I**) in a yield of 93%. The reaction of PdCl₂ with 4-MeOPh-mian in acetonitrile is accompanied by the disproportionation of 4-MeOPh-mian to 4-MeOPh-bian and acenaphthenequinone, and the complex with bis(iminoacenaphthene) [Pd(4-MeOPh-bian)Cl₂] (**II**) is formed (Scheme 2) instead of the expected complex with iminoacenaphthene, which was confirmed by XRD. Complex **II** was synthesized earlier by the direct reaction of PdCl₂ with 4-MeOPh-bian in benzonitrile and crystallized as **II**·1/2C₇H₅N [31]. A similar disproportionation of the iminoacenaphthene is known in the literature. In particular, the formation of the dimeric vanadium complex with 3,5-(CF₃)₂-bian, [$\{VOCl(3,5-(CF_3)_2-Ph-bian)-(H_2O)\}\{VOCl_3(3,5-(CF_3)_2-Ph-bian)\}$], by the reaction of [VO(CH₃CN)₂(H₂O)Cl₂] with 3,5-(CF₃)₂-Ph-mian was reported [14]. In the framework of the present study, compound **II** was obtained as crystals of **II**·C₂H₃N. The synthesis of compounds **I** and **II** is shown in Scheme 2.

The purity of compound **I** was confirmed by elemental and phase XRD analyses (Fig. 1). The purity of complex **II** was confirmed by elemental analysis.

The IR spectrum of compound **I** exhibits intense absorption bands at 1732 and 1622–1579 cm⁻¹ assigned to vibrations of the C=O and C=N bonds of ligand Dpp-mian, respectively, and vibration bands of the C–H bonds of the isopropyl substituents in a range of 2958–2926 cm⁻¹. The IR spectrum of complex **II** contains intense absorption bands at 1635–1502 cm⁻¹ attributed to vibrations of the C=N bond of ligand 4-MeOPh-bian and vibration bands of the C–H bonds in a range of 2960–2833 cm⁻¹.

The molecular structure of compound **I** was determined by XRD. According to the XRD data, compound **I** crystallizes in the triclinic space group $P\bar{1}$ and represents a cocrystallate of two neutral palladium(II) complexes [Pd(Dpp-mian)Cl₂] and [Pd(Dpp-mian)₂Cl₂]. The independent part of the crystalline cell of compound **I** contains one molecule of complex [Pd(Dpp-mian)₂Cl₂] localized in the partial position on the inversion center and one molecule of complex [Pd(Dpp-mian)Cl₂] and one solvate CH₂Cl₂ molecule arranged in the common position. Thus, compound **I** crystallizes as [Pd(Dpp-mian)Cl₂]₂[Pd(Dpp-mian)₂Cl₂]₂·2CH₂Cl₂. The molecular structure of compound **I** is shown in Fig. 2, and selected bond lengths and angles are given in Table 1.

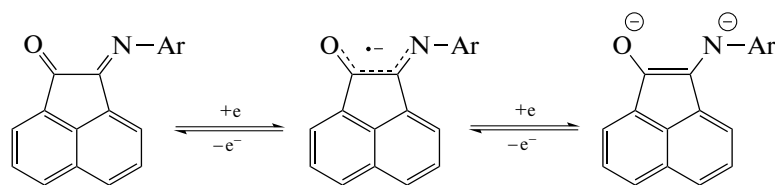


Scheme 2.

The palladium cations in compound **I** have a typical planar square environment. The Pd(1) atom in [Pd(Dpp-mian)Cl₂] is bound to the oxygen and nitrogen atoms of the Dpp-mian ligand and two chlorine atoms. The Pd(1)–N(1) and Pd(1)–O(1) bond lengths are 2.047(2) and 2.096(2) Å, respectively, and the C(1)=N(1), C(1')=O(1), and C(1)–C(1') distances are 1.293(3), 1.239(3), and 1.509(3) Å, respectively, indicating the neutral state of the bidentate-coordinated Dpp-mian ligand. The coordination environment of Pd(2) is formed by two chlorine atoms and two nitrogen atoms of two Dpp-mian ligands. In this case, Dpp-mian acts as a monodentate ligand. The Pd(2)–N(2) bond length is 2.054(2) Å, and the C(2)=N(2), C(2')=O(2), and C(2)–C(2') distances

are 1.286(3), 1.207(3), and 1.564(3) Å, respectively, also indicating that the Dpp-mian ligand exists in the neutral form [13].

Monoiminoacenaphthenones, as well as related bis(iminoacenaphthenes), are redox-active compounds. A possibility of consequent reduction with the formation of the radical-anionic and dianionic species, respectively, was demonstrated for this type of ligands [1, 14]. In addition, deeper reduction processes due to the naphthalene system at potentials significantly shifted to the cathodic region were observed under the electrochemical conditions [1]. The redox transformations of monoiminoacenaphthenones are shown in Scheme 3.



Scheme 3.

The redox properties of compounds **I** and **II** were studied by the CV method using the paste working electrode because of their low solubility in usual organic solvents. The corresponding cyclic voltammograms are shown in Fig. 3, and the potentials are listed

in Table 2. The CV curve of compound **I** is more complicated due to a large set of cathodic and anodic peaks. This is due to the presence of immediately three monoiminoacenaphthenone ligands in compound **I**. According to the structural data, the compound con-

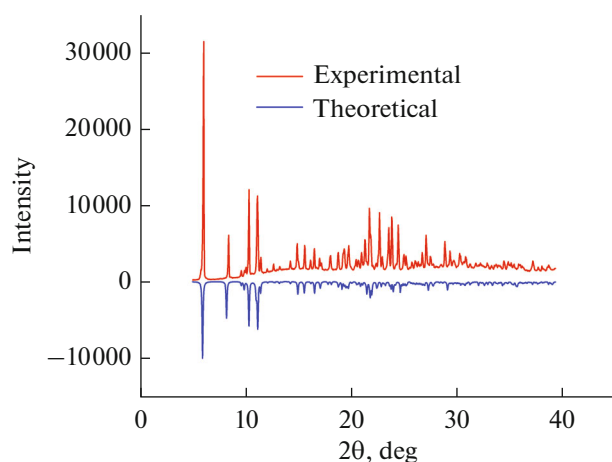


Fig. 1. Powder XRD patterns of complex **I**: theoretical (blue) and experimental (red) patterns.

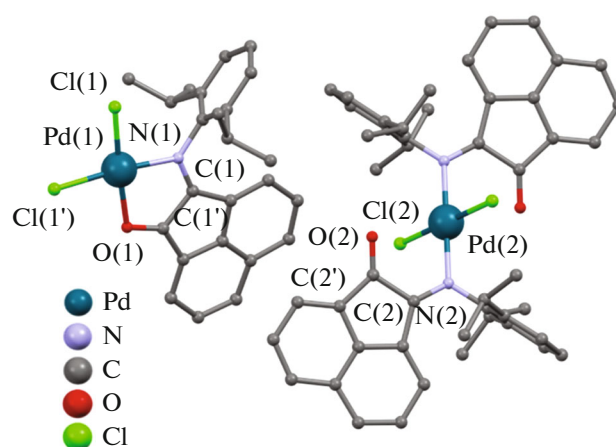


Fig. 2. Molecular structure of compound **I**. Hydrogen atoms and solvate CH_2Cl_2 molecules are omitted.

tains two monodentate-bound and one bidentate-bound Dpp-mian ligands each of which can be reduced in the indicated potential range to form radical-anionic or dianionic species. A similar behavior is confirmed by five peaks (1–5) in the cathodic region from -0.22 to -1.78 V (vs. Ag/AgCl) corresponding to a change in the oxidation state of the ligand. These reduction processes can proceed with the elimination of one or two chloride ligands in each of the $[\text{Pd}(\text{Dpp-mian})\text{Cl}_2]_2$ and $[\text{Pd}(\text{Dpp-mian})_2\text{Cl}_2]$ fragments. This assumption is based on the appearance of anodic peak 12 at 1.12 V characteristic of the oxidation of the free chloride ion [32]. The literature data also indicate the irreversible reduction of resembling complex $[\text{Pd}(\text{Dpp-bian})\text{Cl}_2]$ accompanied by the elimination of the chloride ligands [33].

The CV curves of compound **II** are characterized by a smaller set of redox processes because of only one iminoacenaphthene fragment in its composition. Two main peaks at -0.96 and -1.52 V (peaks 3 and 4) most probably corresponding to the consequent two-electron reduction of 4-MeOPh-bian can be distinguished in the cathodic region. The reduction is most likely accompanied by the elimination of the chloride ligands, which is observed as the appearance of peak 8 at 1.14 V on the anodic branch as in the case of the CV curve of compound **I**. The literature data indicate that resembling in composition and structure complex $[\text{Pd}(\text{Dpp-bian})\text{Cl}_2]$ is reduced at -0.34 and -1.39 V (vs. Ag/AgCl) [33]. The ligand-centered reduction at -1.08 V (vs. Fc^+/Fc) is reported for the $[\text{In}(4-$

Table 1. Selected bond lengths and bond angles in the crystal structure of compound $\text{I} \cdot 2\text{CH}_2\text{Cl}_2$

Bond	$d, \text{Å}$	Angle	deg
Pd(1)–N(1)	2.047(2)	N(1)Pd(1)O(1)	82.05(7)
Pd(1)–O(1)	2.096(2)		
Pd(2)–N(2)	2.054(2)		
Pd(2)–N(3)	2.054(2)		
Pd(1)–Cl(1)	2.2466(7)	N(1)Pd(1)Cl(1)	94.73(6)
Pd(1)–Cl(1')	2.2656(7)	N(1)Pd(1)Cl(1')	173.93(6)
Pd(2)–Cl(2)	2.3093(6)	N(2)Pd(2)Cl(2)	89.96(6)
C(1)–N(1)	1.293(3)		
C(2)–N(2)	1.286(3)		
C(1')–O(1)	1.239(3)		
C(2')–O(2)	1.207(3)		
C(1)–C(1')	1.509(3)		
C(2)–C(2')	1.564(3)		

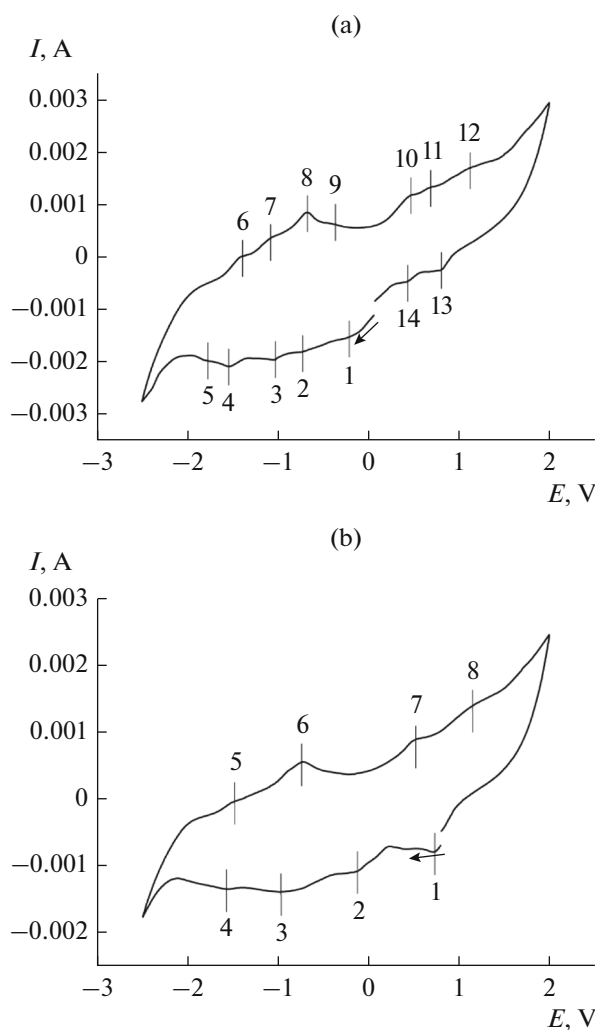


Fig. 3. CV curves of the paste electrode with compounds (a) **I** and (b) **II** (second cycle) in acetonitrile with 0.10 M Bu_4NPF_6 as a supporting electrolyte at a sweep rate of 10 mV/s (cathodic sweep direction).

$\text{MeOPh-bian}_2\text{Cl}_2\text{]Cl}$ indium complex with the 4-MeOPh-bian ligand [34].

Thus, the reactions of PdCl_2 with iminoacenaphthenones were shown to proceed in different ways. In the case of [2,6-diisopropylphenyl]iminoacenaphthene, compound $[\text{Pd}(\text{Dpp-mian})\text{Cl}_2]_2[\text{Pd}(\text{Dpp-mian})_2\text{Cl}_2]$ (**I**) containing two structural units with different coordination modes of Dpp-mian to palladium is formed. On the contrary, the reaction of PdCl_2 with [4-methoxyphenyl]iminoacenaphthene leads to its disproportionation to 1,2-bis[4-methoxyphenyl]iminoacenaphthene and acenaphthenequinone with the further formation of complex $[\text{Pd}(4\text{-MeOPh-bian})\text{Cl}_2]$ (**II**). Compound **I** is the first example of the coordination of the mian type ligand to the palladium ion. Both compounds were found to be prone to mul-

Table 2. Potentials of the processes that occur at the electrode involving compounds **I** and **II**

Compound I		Compound II	
process	potential, V	process	potential, V
Anodic processes			
6	-1.40	5	-1.48
7	-1.08	6	-0.75
8	-0.67	7	0.53
9	-0.36	8	1.14
10	0.47		
11	0.69		
12	1.12		
Cathodic processes			
13	0.80	1	0.73
14	0.43	2	-0.13
1	-0.22	3	-0.96
2	-0.73	4	-1.52
3	-1.03		
4	-1.53		
5	-1.78		

ti-electron reduction due to the presence of the redox-active ligand.

ACKNOWLEDGMENTS

The XRD study of compounds **I** and **II** was carried out using the equipment of the Center for Collective Use "Analytical Center of Institute of Organometallic Chemistry of Russian Academy of Sciences." The authors are grateful to the Ministry of Science and Higher Education of the Russian Federation and the Center for Collective Use at the Nikolaev Institute of Inorganic Chemistry (Siberian Branch, Russian Academy of Sciences).

FUNDING

This work was supported by the Russian Science Foundation, project no. 21-13-00092.

CONFLICT OF INTEREST

The authors of this work declare that they have no conflicts of interest.

REFERENCES

1. Khrizanforova, V.V., Fayzullin, R.R., Gerashimova, T.P., et al., *Int. J. Mol. Sci.*, 2023, vol. 24, no. 10, p. 8667.
2. Razborov, D.A., Lukoyanov, A.N., Baranov, E.V., et al., *Dalton Trans.*, 2015, vol. 44, no. 47, p. 20532.

3. Lukoyanov, A.N., Zvereva, Y.V., Parshina, D.A., et al., *Eur. J. Inorg. Chem.*, 2022, vol. 2022, no. 27, e202200348.
4. Lukoyanov, A.N., Ulivanova, E.A., Razborov, D.A., et al., *Chem.-Eur. J.*, 2019, vol. 25, no. 15, p. 3858.
5. Koptseva, T.S., Moskalev, M.V., Skatova, A.A., et al., *Inorg. Chem.*, 2022, vol. 61, no. 1, p. 206.
6. Bernauer, J., Pölker, J., and von Wangelin, J., *Chem-CatChem*, 2022, vol. 14, no. 1, p. e202101182.
7. Yambulatov, D.S., Nikolaevskii, S.A., Kiskin, M.A., et al., *Molecules*, 2020, vol. 25, no. 9, p. 2054.
8. Romashev, N.F., Bakaev, I.V., Komlyagina, V.I., et al., *J. Struct. Chem.*, 2022, vol. 63, no. 8, p. 1304.
9. Romashev, N.F., Mirzaeva, I.V., Bakaev, I.V., et al., *J. Struct. Chem.*, 2022, vol. 63, no. 2, p. 242.
10. Romashev, N.F., Bakaev, I.V., Komlyagina, V.I., et al., *Int. J. Mol. Sci.*, 2023, vol. 24, no. 13, p. 10457.
11. Komlyagina, V.I., Romashev, N.F., Besprozvannykh, V.K., et al., *Inorg. Chem.*, 2023, vol. 62, no. 29, p. 11541.
12. Razborov, D.A., Lukoyanov, A.N., Makarov, V.M., et al., *Russ. Chem. Bull.*, 2015, vol. 64, no. 10, p. 2377.
13. Anga, S., Paul, M., Naktode, K., et al., *Z. Anorg. Allg. Chem.*, 2012, vol. 638, no. 9, p. 13115.
14. Lukoyanov, A.N., Fomenko, I.S., Gongola, M.I., et al., *Molecules*, 2021, vol. 26, no. 18, p. 5706.
15. Anga, S., Pal, T., Kottalanka, R.K., et al., *Can. Chem. Trans.*, 2013, vol. 1, no. 2, p. 105.
16. Anga, S., Rej, S., Naktode, K., et al., *J. Chem. Sci.*, 2015, vol. 127, no. 1, p. 103.
17. Gao, B., Gao, W., Wu, Q., et al., *Organometallics*, 2011, vol. 30, no. 20, p. 5480.
18. Carrington, S.J., Chakraborty, I., and Mascharak, P.K., *Dalton Trans.*, 2015, vol. 44, no. 31, p. 13828.
19. Hazari, A.S., Das, A., Ray R., et al., *Inorg. Chem.*, 2015, vol. 54, no. 10, p. 4998.
20. Visentin, L.C., Ferreira, L.C., Bordinhão, J., et al., *J. Braz. Chem. Soc.*, 2010, vol. 21, no. 7, p. 1187.
21. Bhattacharjee, J., Sachdeva, M., Banerjee, I., et al., *J. Chem. Sci.*, 2016, vol. 128, no. 6, p. 875.
22. Singha Hazari, A., Ray, R., Hoque, M.A., et al., *Inorg. Chem.*, 2016, vol. 55, no. 16, p. 8160.
23. Tang, X., Huang, Y.T., Liu, H., et al., *J. Organomet. Chem.*, 2013, vol. 729, p. 95.
24. Fomenko, I.S., Nadolinny, V.A., Efimov, N.N., et al., *Russ. J. Coord. Chem.*, 2019, vol. 45, p. 776. <https://doi.org/10.1134/S1070328419110022>
25. Komlyagina, V.I., Romashev, N.F., Kokovkin, V.V., et al., *Molecules*, 2022, vol. 27, no. 20, p. 6961.
26. Kuznetsova, A.A., Volchek, V.V., Yanshole, V.V., et al., *Inorg. Chem.*, 2022, vol. 61, no. 37, p. 14560.
27. *APEX3. SAINT*, Madison: Bruker AXS Inc., 2018.
28. Krause, L., Herbst-Irmer, R., Sheldrick, G.M., and Stalke, D., *J. Appl. Crystallogr.*, 2015, vol. 48, no. 1, p. 3.
29. Sheldrick, G.M., *Acta Crystallogr., Sect. C: Struct. Chem.*, 2015, vol. 71, p. 3.
30. Sheldrick, G.M., *Acta Crystallogr., Sect. A: Found. Adv.*, 2015, vol. 71, no. 1, p. 3.
31. Coventry, D.N., Batsanov, A.S., Goeta, A.E., et al., *Polyhedron*, 2004, vol. 23, no. 17, p. 2789.
32. Romashev, N.F., Gushchin, A.L., Fomenko, I.S., et al., *Polyhedron*, 2019, vol. 173, p. 114110.
33. Romashev, N.F., Abramov, P.A., Bakaev, I.V., et al., *Inorg. Chem.*, 2022, vol. 61, no. 4, p. 2105.
34. Wang, J., Ganguly, R., Yongxin, L., et al., *Dalton Trans.*, 2016, vol. 45, no. 19, p. 7941.

Translated by E. Yablonskaya

Publisher's Note. Pleiades Publishing remains neutral with regard to jurisdictional claims in published maps and institutional affiliations.